

1 **SLRfinder: a method to detect candidate sex-linked regions with linkage disequilibrium**
2 **clustering**

3 Running title: Detect sex-link regions using population genomics

4

5 Xueling Yi^{1*}, Petri Kemppainen^{1*}, Juha Merilä^{1,2}

6 ¹ Area of Ecology and Biodiversity, School of Biological Sciences, The University of Hong Kong,
7 Hong Kong SAR

8 ² Ecological Genetics Research Unit, Organismal and Evolutionary Biology Programme, University
9 of Helsinki, FI-00014 University of Helsinki, Finland

10 * these authors contributed equally

11

12 Corresponding authors:

13 Xueling Yi (xlyi@hku.hk) & Petri Kemppainen (peke@hku.hk)

14

15 **Abstract**

16 Despite their critical roles in genetic sex determination, sex chromosomes remain unknown in many
17 non-model organisms. In contrast to conserved sex chromosomes in mammals and birds, studies of
18 fish, amphibians, and reptiles have found highly labile sex chromosomes with newly evolved sex-
19 linked regions (SLRs). These labile sex chromosomes are important for understanding early sex
20 chromosome evolution but are difficult to identify due to the lack of Y/W degeneration and SLRs
21 limited to small genomic regions. Here we present SLRfinder, a method to identify candidate SLRs
22 and labile sex chromosomes using linkage disequilibrium (LD) clustering, patterns of heterozygosity,
23 and genetic divergence. SLRfinder does not rely on specific sequencing methods or reference
24 genomes and does not require phenotypic sexes which may be unknown from population sampling,
25 although sex information can be incorporated to provide additional inference on candidate SLRs. We
26 tested SLRfinder using various published datasets and compared it to SATC, a method that identifies
27 sex chromosomes based on the depth of coverage and also does not require phenotypic sex. Results
28 show that SATC works better on conserved sex chromosomes (e.g., in African leopards), whereas
29 SLRfinder outperforms SATC in analyzing labile sex chromosomes (e.g., in nine-spined sticklebacks)

30 and chum salmon). Since SLRfinder primarily relies on LD clusters, it is expected to be most
31 sensitive to the SLRs harboring structural variants (e.g., inversion) due to strongly reduced
32 recombination rates in heterozygotes. SLRfinder provides a novel and complementary approach for
33 identifying SLRs and uncovering additional sex chromosome diversity in nature.

34

35 **Key words**

36 Heterozygosity, Inversion, LD, Sex chromosomes, Sex-determining region, SLR

37

38 **Introduction**

39 Sex chromosomes play critical roles in genetic sex determination and yet remain unknown in many
40 non-model organisms. Early studies in mammals and birds have demonstrated highly conserved and
41 heteromorphic (i.e., having different morphologies) sex chromosomes with conserved sex-
42 determining genes and degenerated Y or W chromosomes. On the other hand, accumulating studies
43 have found less conserved but much more labile sex chromosomes that may be different between
44 closely related lineages in fish, amphibians, and reptiles (Dufresnes et al., 2015; Jeffries et al., 2018;
45 Yi et al., 2024). These labile sex chromosomes tend to be homomorphic (i.e., sex chromosomes
46 having indistinguishable morphologies) and are featured by little or no degeneration, low inter-sex
47 differentiation, variable sex-determining genes, and sex-determining regions restricted to narrow
48 genomic regions. These features make labile sex chromosomes and their sex-determining regions
49 difficult to identify using traditional methods such as karyotyping and PCR of conserved sex-
50 determining genes (Palmer et al., 2019; Tree of Sex Consortium, 2014). However, labile sex
51 chromosomes likely represent early evolutionary stages of sex chromosome evolution and their study
52 is critical for our understanding of sex chromosome evolution (Blaser et al., 2014; Furman et al.,
53 2020; Perrin, 2021; Vicoso, 2019). Therefore, additional work is needed to identify labile sex
54 chromosomes and their sex-determining regions in non-model species.

55 Recently, several methods have been developed to help identify sex chromosomes and their sex-
56 determining regions in non-model species, but these methods mostly work for conserved sex
57 chromosomes and are limited to certain types of sequencing data. For example, RADSex (Feron et al.,
58 2021) was developed to identify sex determination systems (i.e., XX/XY or ZZ/ZW) and sex-linked
59 markers of labile sex chromosomes specifically from restriction site-associated DNA sequencing
60 (RADseq) data, and Pooled Sequencing Analysis for Sex Signal (PSASS ver. 3.1.0;
61 <https://github.com/SexGenomicsToolkit/PSASS>) was developed to detect sex-linked signals using

62 pooled sequencing data from males and females (e.g., in Kitano et al., 2023). These methods are not
63 applicable to whole-genome sequencing (WGS) data which has been increasingly used in studies of
64 non-model populations. In addition, these methods require known phenotypic sexes which may not be
65 available in non-invasive sampling or may be difficult to identify in individuals that are not sexually
66 mature or have limited or no sexual dimorphism. FindZX (Sigeman et al., 2022) was developed to
67 detect sex chromosomes using WGS data. This method has been applied to diverse systems including
68 both conserved and labile sex chromosomes, and it can work on very small sample sizes (Sigeman et
69 al., 2022). However, this method also relies on known phenotypic sexes, and it requires a reference
70 genome of the homogametic sex (i.e., XX female or ZZ male) which may not be available or may be
71 unknown if the sex determination system is unclear. SATC (Sex Assignment Through Coverage;
72 Nursyifa et al., 2022) was developed to jointly identify sex chromosomes and genetic sex using WGS
73 data. This method does not require known phenotypic sexes, but it assumes that only X/Z scaffolds
74 are assembled in the reference genome, which is practically the same as requiring a reference genome
75 of the homogametic sex. In addition, the available methods are mostly based on sequencing depth
76 (RADSex and SATC) or depth and heterozygosity (PSASS, FindZX), but many studies have shown
77 that depth may not differ between sexes on labile sex chromosomes which are homomorphic with
78 narrow sex-determining regions (Jeffries et al., 2022; Yi et al., 2024). Therefore, new methods are
79 needed to help identify labile sex chromosomes in non-model populations.

80 A previous study has shown that LD can be a signal for detecting sex-determining regions (McKinney
81 et al., 2020). Here we present a method (herein SLRfinder) to identify candidate sex-linked regions
82 (SLRs) among clusters of highly correlated SNPs (LD clusters) based on the differentiation in
83 heterozygosity and the genetic differentiation captured by Principal Component Analysis (PCA). The
84 identified candidate SLRs should include the sex-determining region and its linked genomic regions
85 on sex chromosomes, as well as possible rare sex-linked autosomal regions. However, the sex-
86 determining region is expected to have the strongest signal of LD due to recombination suppression
87 between sex chromosomes, and the clearest genetic divergence between sexes captured by PCA. The
88 heterozygosity difference in the sex-determining region can be used to indicate homogametic and
89 heterogametic sexes. SLRfinder is expected to outperform the coverage-based methods in identifying
90 young sex chromosomes, and it does not rely on specific types of sequencing methods or reference
91 genomes. Like SATC, SLRfinder does not require phenotypic sexes, although known sex information
92 can be incorporated as a complementary filtering to provide additional inference for candidate sex
93 chromosomes.

94 Below we describe the workflow of SLRfinder and its application to published datasets of various
95 taxa having identified labile sex chromosomes, including nine-spined sticklebacks (*Pungitius*
96 *pungitius*), chum salmon (*Oncorhynchus keta*), and guppies (*Poecilia reticulata*). We also tested the

97 effectiveness of SLRfinder in conserved sex chromosomes using a dataset of African leopards
98 (*Panthera pardus*). In addition, we compared the performance of SLRfinder to SATC, the only other
99 method that does not require known phenotypic sexes. Results show that, as expected, SATC only
100 worked on conserved sex chromosomes and might yield wrong sex inferences when using a reference
101 genome of the heterogametic sex. On the other hand, SLRfinder does not rely on specific types of
102 reference genomes and it outperforms SATC in analysing labile sex chromosomes, especially when
103 the SLR is associated with genomic inversions. Since SLRfinder and SATC are based on independent
104 signals (i.e., LD and heterozygosity versus depths of coverage), they are complementary to each other
105 and should thus be considered jointly to maximize the ability to identify sex chromosomes in non-
106 model species.

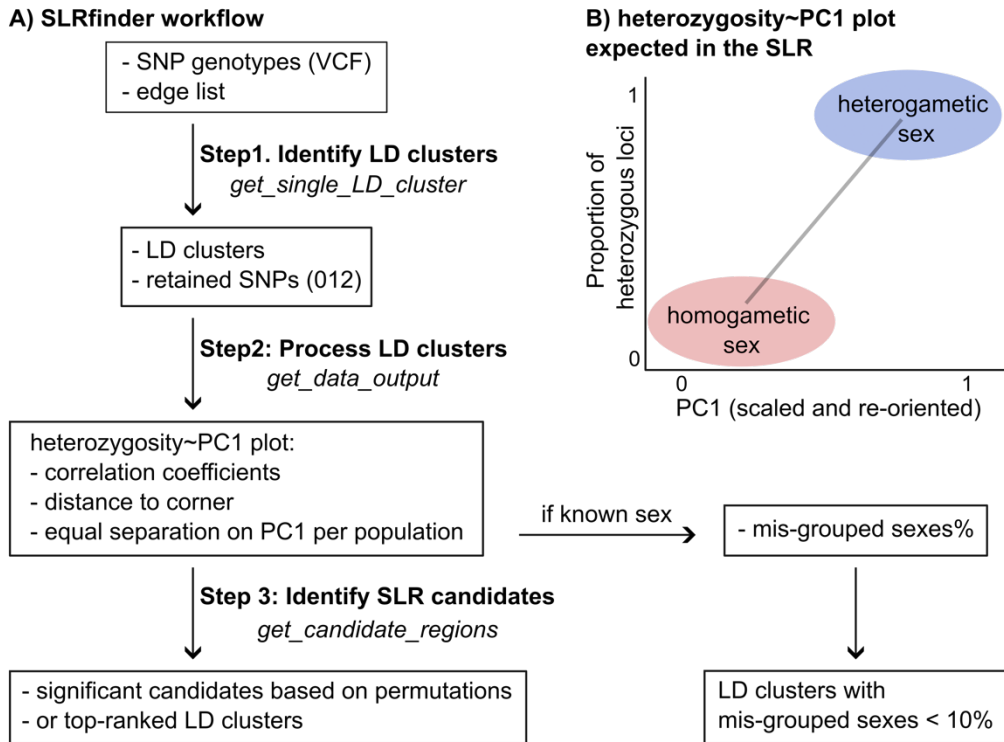
107

108 Materials and Methods

109 Identify LD clusters from VCF inputs

110 The workflow of SLRfinder is summarized in **Figure 1**. The input data is a VCF file of filtered
111 biallelic single nucleotide polymorphisms (SNPs) from populations genotyped using WGS or
112 reduced-representation sequencing methods (e.g., RADseq). LD is estimated in VCFtools (Danecek et
113 al., 2011) as squared coefficient of correlation (r^2) between pairs of loci within windows of 100 SNPs
114 (--geno-r2 --ld-window 100). In a network analytical framework (Kemppainen et al., 2015), LD
115 clusters are identified by only considering LD values (edges) with $r^2 > min_LD$ (default 0.85) between
116 pairs of loci (nodes). The resulting edge list (each row corresponding to a locus pair with $r^2 > min_LD$)
117 is used to generate a “graph object” using the function *graph.edgelist* from the package *igraph* (Csardi
118 et al., 2006) in R v4 (R Core Team, 2022). The graph object is further decomposed into separate LD
119 clusters that are not connected by any edges using the function *decompose.graph*. The resulting LD
120 clusters are defined by their weakest edges such that only loci belonging to the same cluster can be
121 connected by $r^2 > min_LD$ (i.e. single linkage clustering). Finally, only clusters with a minimum of
122 *min.cl.size* loci (default 20) are retained for downstream analyses.

123



124

125 **Figure 1. The workflow of SLRfinder. A)** The three major steps of SLRfinder. **B)** Illustration of the
126 expected heterozygosity~PC1 plot in the SLR.

127

128 *Estimating heterozygosity and conducting PCA in each LD cluster*

129 All SNPs from each identified LD cluster are used to conduct a PCA using the R package SNPRelate
130 (Zheng et al., 2012) and estimate the observed heterozygosity as the proportion of heterozygous SNPs
131 (coded as 1 in the 012 file) in the non-missing SNPs genotyped in each individual. A linear model is
132 fitted to regress the estimated individual heterozygosity on scaled PC1 (also polarized if the original
133 relationship is negative). The heterozygosity~PC1 plots are expected to show no grouping pattern in
134 most LD clusters, three groups in a triangular shape representing three genotypes in autosomal
135 inversions (Ma & Amos, 2012), and two groups corresponding to the homogametic sex (bottom-left
136 corner) and the heterogametic sex (top-right corner) in SLRs (Fig. 1B). Accordingly, candidate SLRs
137 are expected to have stronger association between heterozygosity and PC1, and stronger inter-sex
138 genetic divergence than population structure captured on PC1. Based on these expectations, we
139 estimate the adjusted R-squared values of the linear regressions and the χ^2 goodness-of-fit tests on an
140 equal separation of samples in each population on PC1 under the assumption of an equal sex ratio and
141 random sampling. Smaller χ^2 statistics indicate that all populations include individuals from both
142 groups, therefore indicating potentially stronger inter-sex differentiation than population structure in
143 this region. If in some cases skewed sex ratios are expected, the expected probabilities of sampling the

144 heterogametic sex and the homogametic sex can be provided to get more accurate χ^2 estimates. In
145 addition, we estimated the scaled Euclidean distance between each individual and its nearest corner
146 individual (i.e., the individuals having the highest or lowest heterozygosity, and if equal
147 heterozygosity the highest or lowest scaled PC1 scores). Assuming no recombination, candidate SLRs
148 are expected to have a clear and strong separation between groups on the heterozygosity~PC1 plot,
149 resulting in shorter Euclidean distances with smaller variance.

150 *Identify SLR candidates*

151 Candidate SLRs are identified among LD clusters based on their ranks of the estimated parameters. A
152 LD cluster is ranked higher (i.e., more likely to be a SLR) if it has more SNPs, stronger
153 heterozygosity~PC1 regression, smaller variation of the Euclidean distance (i.e., better grouping on
154 the heterozygosity~PC1 plot), and smaller χ^2 statistic (i.e., roughly equal separation of individuals per
155 population on PC1). The summed ranks of these parameters are permuted (default 10000 times)
156 among LD clusters to generate a null-distribution of the summed ranks and estimate how often the
157 permuted values are lower than the observed value (i.e., the p -value) of each LD cluster. In addition,
158 we correct potential p -value inflation using genomic control (Devlin et al., 2001; Devlin & Roeder,
159 1999). Briefly, the $-\log_{10}(p)$ values are divided by the inflation factor (λ) estimated as the linear slope
160 in a quantile-quantile plot between the observed $-\log_{10}(p)$ and those expected under the null-
161 hypothesis of a uniform distribution of p -values. Significant (adjusted p -value < 0.05) candidates (or
162 the five top-ranked LD clusters if no significance) are reported with their heterozygosity~PC1 plots.

163 Although SLRfinder does not require phenotypic sexes, known sex information can be incorporated to
164 filter LD clusters where the two sexes are fully separated on the heterozygosity~PC1 plot, which can
165 provide additional inference on candidate sex chromosomes. To do this, we estimate the percentage of
166 sexed individuals that are likely placed in the wrong group (i.e., the minority sex in a group is
167 regarded as misplaced), and filter the LD clusters that have less than 10% mis-placed individuals
168 (allowing for rare phenotypic misidentifications).

169 *Test of SLRfinder using published datasets*

170 To test the efficiency and accuracy of SLRfinder, we applied it to published empirical datasets of
171 various species (**Table S1**). First, we applied SLRfinder to the nine-spined stickleback (*Pungitius*
172 *pungitius*) lineages that have different sex chromosomes. Previous studies have shown that the non-
173 European and Eastern European (EL) lineages have heteromorphic sex chromosomes identified as
174 LG12, whereas the Western European lineage (WL) have homomorphic sex chromosomes identified
175 as LG3, and two UK populations have unidentified sex chromosomes (Dixon et al., 2019; Natri et al.,
176 2019; Yi et al., 2024). The WGS data of nine-spined sticklebacks were published in a previous study

177 (Feng et al., 2022) and available on ENA (project PRJEB39599). The raw sequencing data were re-
178 mapped to the version 7 reference genome of *Pungitius pungitius* (GCA_902500615.3; Kivikoski et
179 al., 2021) using bwa-mem in BWA v0.7.17 (Li, 2013), sorted and indexed using SAMtools version
180 1.16.1 (Danecek et al., 2021), and genotyped by Genome Analysis Toolkit (GATK) following the best
181 practice protocol (Depristo et al., 2011; Van der Auwera et al., 2013). Biallelic SNPs were extracted
182 using the commands -m2 -M2 -v snps -min-ac=1 in BCFtools (Li, 2011) and data mapped to
183 unassembled contigs were removed. The SNP genotypes were split into four datasets representing the
184 WL, the EL, the non-European lineage, and the UK lineage. Each dataset was further filtered in
185 VCFtools by quality (--minGQ 20 --minQ 30), missing data (--max-missing 0.75), and minor allele
186 frequency (--maf 0.15) before analysed by SLRfinder. The same filtering was used below in the other
187 test datasets. Phenotypic sexes are known in one EL and one WL population and were provided to
188 SLRfinder.

189 Next, we applied SLRfinder to chum salmon (*Oncorhynchus keta*) whose sex chromosomes have
190 been identified as LG15 in studies using RADseq (McKinney et al., 2020) or WGS data (Rondeau et
191 al., 2023). We re-analysed both datasets using SLRfinder. The WGS data were mapped to the newly
192 assembled male reference genome of *Oncorhynchus keta* (GCF_023373465.1) and the VCF file of
193 genotyped bi-allelic SNPs were downloaded from the corresponding publication (Rondeau et al.,
194 2023) and filtered before being analysed by SLRfinder. In addition, to test the potential influence of
195 different reference genomes, we downloaded the raw WGS data from NCBI (BioProject
196 PRJNA556729), mapped them to a female reference genome (GCF_012931545.1), and genotyped
197 and filtered SNPs in the same way described above. To test the application of SLRfinder on reduced-
198 representation sequencing data, we also re-analysed the RADseq data published in (McKinney et al.,
199 2020). The demultiplexed raw sequencing data were downloaded from NCBI (BioProject
200 PRJNA611968) and mapped to the male reference genome (GCF_023373465.1) using bwa-mem. The
201 mapped reads were sorted, indexed, and marked with duplicates using SAMtools and genotyped using
202 the program *ref_map.pl* with default settings in Stacks 2.65 (Rochette et al., 2019). The genotyped
203 data were further filtered using the program *populations* by minor allele frequency (--min-maf 0.15)
204 and missing data (-R 0.75), and the ordered genotypes were output in the VCF format. We did not
205 output a single SNP per stack locus as the following analyses are based on the information of linkage
206 disequilibrium. The output VCF file was analysed by SLRfinder using a lower threshold for detecting
207 LD clusters (*min_LD*=0.2, *min.cl.size*=5) due to lower SNP density in RADseq data. Phenotypic sexes
208 are known for the WGS dataset (Rondeau et al., 2023) but not the RADseq dataset (McKinney et al.,
209 2020).

210 We also applied SLRfinder to datasets of guppies (*Poecilia reticulata*) whose sex chromosomes have
211 been identified as the LG12 with two SLR candidates indicated using a newly assembled male

212 reference genome (Fraser et al., 2020). The raw WGS data of previously studied populations (Fraser
213 et al., 2020; Kü Nstner et al., 2016) were downloaded from NCBI (BioProject PRJEB10680,
214 PRJNA238429) and mapped separately to the male reference genome (GCA_904066995.1) and a
215 female reference genome (GCA_000633615.2) to test potential impacts of using different references.
216 Data mapping, genotyping, and SNP filtering were done in the same way as in nine-spined
217 sticklebacks. Phenotypic sexes are known for these individuals (Fraser et al., 2020) and were provided
218 to SLRfinder.

219 Lastly, we applied SLRfinder to African leopards (*Panthera pardus*) which have conserved sex
220 chromosomes. Due to computational constraints, we only analysed the WGS data of 26 individuals
221 published in a previous study (Pečnerová et al., 2021). The raw data were downloaded from NCBI
222 (BioProject PRJEB41230) and mapped to a scaffold-level female reference genome of *Panthera*
223 *pardus* (GCF_001857705.1). Data mapping, genotyping, and SNP filtering were done in the same
224 way as in nine-spined sticklebacks. Because sample populations are not provided for the raw
225 sequencing data on NCBI, we assigned these individuals into genetic populations based on PCA using
226 separately filtered biallelic SNPs (--minGQ 20 --minQ 30 --maf 0.05 --max-missing 0.8). No
227 phenotypic sexes were provided and the genetic sexes inferred by SATC (see below) were used as the
228 sex information in SLRfinder.

229 *Identifying sex and SLRs using SATC*

230 We also compared the effectiveness of SLRfinder to SATC (Nursyifa et al., 2022) using the above
231 datasets, excluding the salmon WGS data mapped to the male reference genome because this dataset
232 was a VCF file downloaded from the previous publication (Rondeau et al., 2023) and the bam files
233 were not available. To run SATC, the depth of coverage was calculated by SAMtools-idxstats using
234 the mapped and duplicates-marked individual bam files. Then the idx files were processed by SATC
235 with default settings which filter scaffolds by minimum 100kb, normalize length by the five longest
236 scaffolds, and identify sex scaffolds by the Gaussian model.

237 *Testing the power of SLRfinder using different sample sizes and sex ratios*

238 To assess the statistical power of SLRfinder, we applied it to subsets of the WL and EL nine-spined
239 stickleback datasets where we varied the number of individuals or populations and tested uneven sex
240 ratios. To test effects of sample sizes, we first randomly selected 3-5 individuals per population while
241 including all populations in the WL or EL dataset. Then we randomly selected 1-5 WL or EL
242 populations while including all individuals from the selected populations. To test effects of sex ratios,
243 we used the previously identified genetic sexes of these individuals (Yi et al., 2024) and only included
244 the seven WL populations and the 24 EL populations that have at least 4 individuals per sex. We

245 randomly selected 2 individuals per sex per population (even sex ratio), or 1 individual from one sex
246 and 3 from the other in each population (sex ratios 1:3 or 3:1). To test sex ratios 1:2 or 2:1, we
247 randomly selected 9 individuals from one sex and 19 from the other across WL populations, and 32
248 individuals from one sex and 64 from the other across EL populations. To test sex ratios 1:10 or 10:1,
249 we randomly selected 3 individuals from one sex and 25 from the other across WL populations, and 9
250 individuals from one sex and 87 from the other across EL populations. We also tested extreme
251 scenarios where only one sex was sampled in the dataset. The subset VCF files of the selected
252 individuals were filtered and processed by SLRfinder as described above. We first used the default
253 expectation of an equal sex ratio in all tests. When the true SLR was not included in top-ranked
254 candidates, we further modified the parameters to rank and the expected sex ratios in the χ^2 tests to see
255 if SLRfinder results can be improved.

256

257 **Results**

258 *SLRfinder analyses of nine-spined sticklebacks and chum salmon*

259 SLRfinder successfully identified the sex chromosomes and SLRs of nine-spined sticklebacks (Table
260 1; Fig. 2). In the WL dataset, SLRfinder identified a single significant candidate on LG3 that highly
261 overlaps with the previously described WL SLR (LG3:17260000-17340000 bp; Yi et al., 2024).
262 Similarly, in the EL and non-European datasets, SLRfinder identified a single significant candidate on
263 LG12 that highly overlaps with the previously reported EL SLR (LG12:1-16900000 bp (Kivikoski et
264 al., 2021). The SLRfinder-inferred genetic sexes are also consistent with known phenotypic sexes and
265 the previous identifications of genetic sex (Yi et al., 2024). The UK dataset did not generate
266 significant candidates, possibly due to the limited power of SLRfinder on small sample sizes (see
267 below). However, none of the top-ranked candidates were located on LG12 or LG3 (Table S1),
268 consistent with the previous findings that sex chromosomes of the UK populations are likely neither
269 LG12 nor LG3 (Yi et al., 2024). Instead, the LD clusters having the lowest adjusted *p*-values
270 (*p*=0.2179) included a 225-bp region on LG7 and a 203-bp region on LG16 (Table 1, Fig. S1A).
271 Additional sampling of individuals with known sexes is required to validate if these regions can
272 separate the two sexes and to identify the yet unknown sex chromosomes of the UK populations.

273

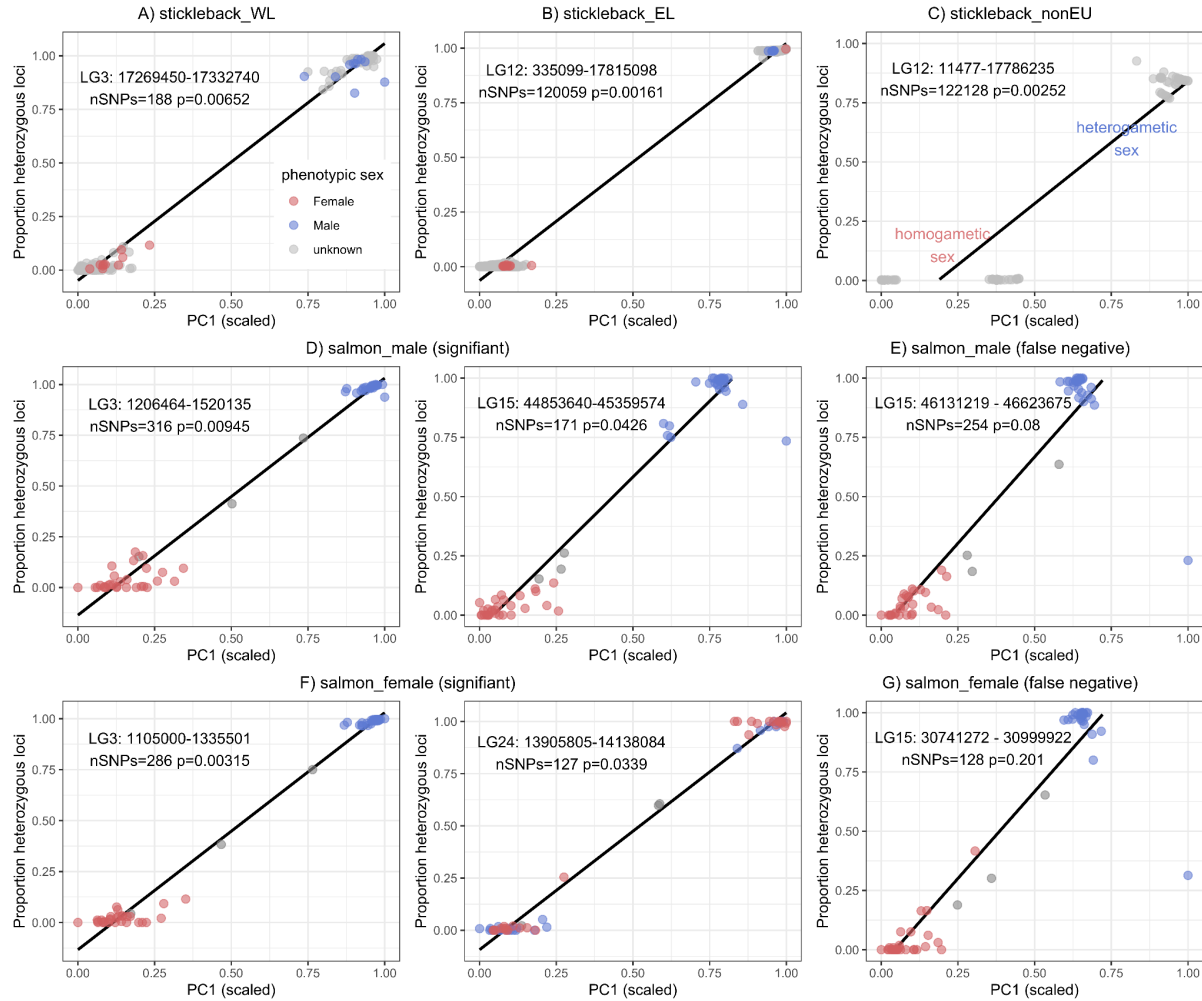
274 **Table 1. Summary of the SLRfinder results using test datasets.** Sex-filtered results are the LD
275 clusters having less than 10% misplaced sexed individuals. Ranked candidates are the LD clusters
276 tested significant (adjusted *p* < 0.05) or, if non-significant, the clusters having the lowest adjusted *p*-

277 value (only those with $p < 0.5$ are listed). Clusters on the known sex chromosomes are indicated in
278 bold.

Dataset	# Ind	# Pop	# LD cluster	Sex_filter	Rank_candidates
stickleback_WL	162	8	2737	LG3 (1 cluster)	LG3: 17269450-17332740
stickleback_EL	598	29	1149	LG12 (6 clusters)	LG12: 335099-17815098
stickleback_nonEU	78	5	1329	Sex unknown	LG12:11477-17786235
stickleback_UK	29	2	5331	Sex unknown	LG7: 3628961-3664806, LG16: 12008573-12103926 ($p = 0.2179$)
salmon_male	59	11	25646	LG3 (2 clusters), LG15 (2 clusters)	LG3: 1206464-1520135, LG15: 44853640-45359574
salmon_female	59	11	28294	LG3 (2 clusters), LG15 (3 clusters), LG26 (2 clusters), LG32 (1 cluster)	LG3:1105000-1335501, LG24:13905805-14138084
salmon_RAD	288	6	1498	Sex unknown	LG14: 53640831-53640941, LG15: 22646022-46527777 ($p = 0.06$)
guppy_female	170	10	103	No cluster retained.	All clusters had $p > 0.5$
guppy_male	170	10	78	No cluster retained.	All clusters had $p > 0.5$
leopard	26	3	90	NW_017619865.1 NW_017619916.1 NW_017619950.1 NW_017619951.1 NW_017619964.1 NW_017620089.1	All clusters had $p > 0.5$

279

280



281

282 **Figure 2. The heterozygosity-PC1 plot of the SLRfinder-identified candidates using datasets of**
283 **nine-spined sticklebacks (A-C) and chum salmon (D-G). Dots represent individuals colored by the**
284 **phenotypic sex. The black line represents the fitted linear regression. B) The single phenotypic female**
285 **in the top-right group is the individual 16-f that was also found to be a genetic male in previous**
286 **studies (Feng et al., 2022; Yi et al., 2024). E & G) The false negative clusters on LG15 detected by**
287 **the sex percent filtering. Two more false negatives were detected in the salmon_female dataset but**
288 **had much fewer SNPs (nSNPs of 26 and 96) and thus were not plotted.**

289

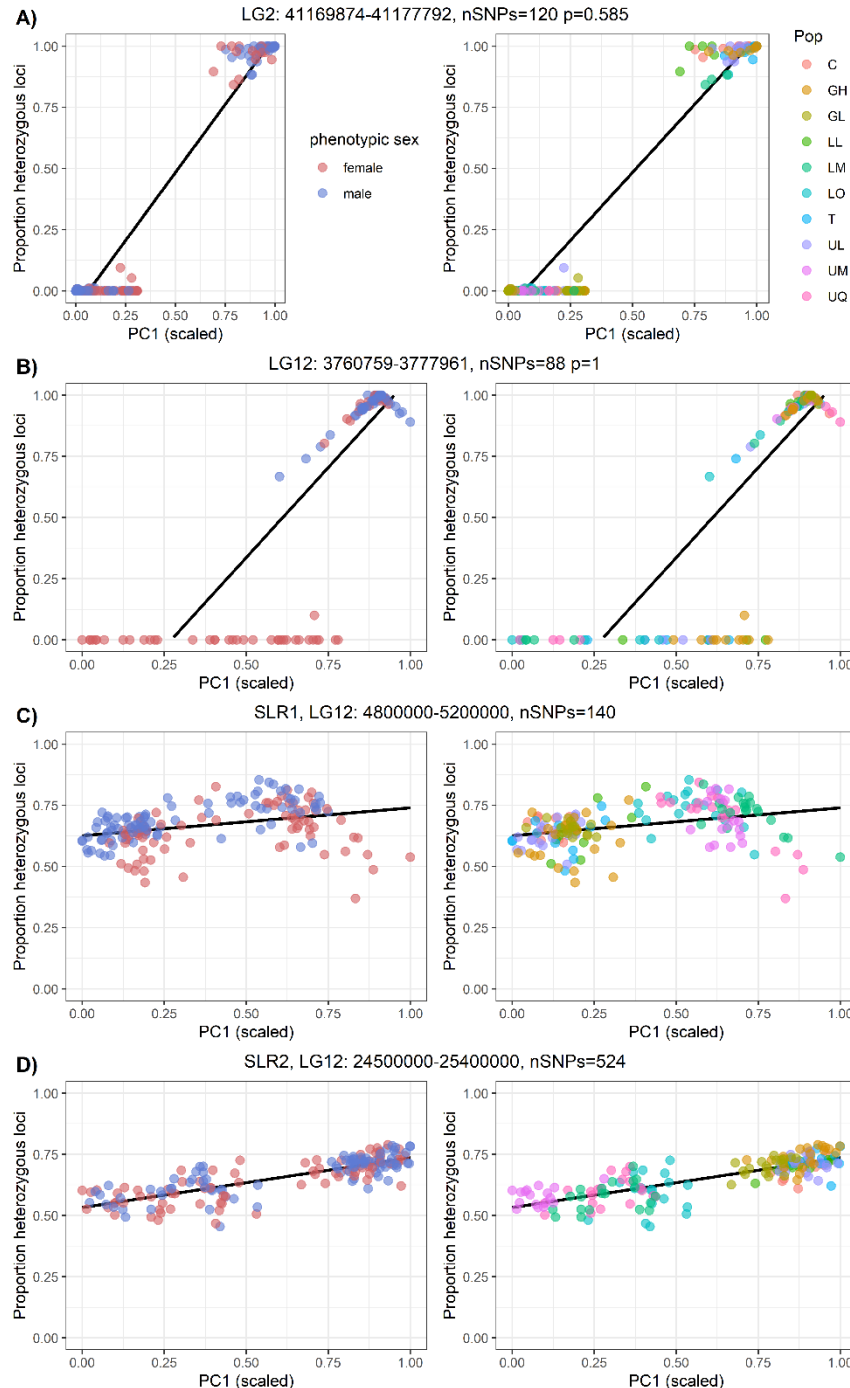
290 SLRfinder also identified the sex chromosomes and SLRs of chum salmon (Table 1; Fig. 2). When
291 using the WGS data mapped to the male reference, SLRfinder identified LG15 and LG3 as significant
292 candidates, both highly overlapping with the previously reported sex-associated regions
293 (LG3:750001-1950001, LG15:40010001-46610001, and LG26:1-280001) in Genome-Wide
294 Association Studies (GWAS; Rondeau et al., 2023). Because LG15 was inferred as sex chromosomes
295 by independent studies using different datasets and analyses (McKinney et al., 2020; Rondeau et al.,
296 2023), the LG3 cluster most likely represents a true sex-linked autosomal region. Interestingly,

297 despite the complete separation between two sexes on the heterozygosity~PC1 plot of this LG3
298 cluster, the few individuals of unknown sex were not grouped with either sex in the LG3 cluster but
299 were clearly grouped with females in the significant LG15 cluster which is the true SLR (Fig. 2D).
300 Another LG15 cluster located within the previously identified SLR (LG15:40010001-46610001;
301 Rondeau et al., 2023) was also detected by filtering the percentage of misplaced sexes. Therefore, this
302 cluster was a false negative ($p=0.08$) with a marginal rank probably due to an outlier male individual
303 on the heterozygosity~PC1 plot (Fig. 2E). Similarly, when using the WGS data mapped to the female
304 reference, the autosomal LG3 cluster was identified significant and three LG15 clusters were detected
305 by filtering the misplaced sexes but were ranked as false negatives ($p>0.2$) probably due to an outlier
306 male that had relatively low heterozygosity (Fig. 2FG, Table 1, Table S1). On the other hand,
307 SLRfinder identified a false positive ($p=0.03$) LG24 cluster which showed a similar pattern but did
308 not separate two sexes on the heterozygosity~PC1 plot (Fig. 2F). When using the RADseq data, no
309 significant candidate was identified but the true LG15 SLR was the top-ranked cluster having 319
310 SNPs and a marginal p -value of 0.06 (Table 1). This false negative result was possibly due to the
311 sparse RADseq SNPs and loose LD filtering ($\text{min_LD}=0.2$) of this dataset which generated a weak
312 grouping on the heterozygosity~PC1 plot (Fig. S1B).

313 *SLRfinder analyses of guppies and leopard*

314 SLRfinder did not identify significant candidates using the datasets of guppies (Table 1). Previous
315 studies have identified LG12 as the sex chromosomes of guppies (Fraser et al., 2020). However, none
316 of the top-ranked clusters were located on LG12 (Table S1, Fig. 3A, Fig. S2A). In fact, despite a
317 relatively large sample size (170 individuals, 10 populations), the guppy datasets were identified with
318 very few LD clusters (Table 1) including only two LG12 clusters using the female reference genome
319 (Fig. S2BC) and one LG12 cluster using the male reference genome (Fig. 3B), none of which showed
320 a separation between sexes. To further investigate the signal of SLRs in guppies, we extracted SNPs
321 located in the previously reported candidate SLRs (LG12: 4800000-5200000 bp, LG12: 24500000-
322 25400000 bp) using the filtered VCF mapped to the male reference genome that was used to identify
323 these SLRs (Fraser et al., 2020). For each SLR, all SNPs were used to generate the
324 heterozygosity~PC1 plot, which showed similar heterozygosity in males and females and stronger
325 population structure than sex differentiation on PC1 (Fig. 3CD). Therefore, these results indicate that
326 the guppy datasets do not have the expected signal for SLRs (i.e., inter-sex differentiation in
327 heterozygosity and stronger differentiation between sexes than population structure on PC1), which
328 explains why SLRfinder was not able to identify these SLRs.

329



330

331 **Figure 3. The heterozygosity~PC1 plots of the guppy dataset mapped to the male reference**
332 **genome.** Each dot is one individual colored by phenotypic sex (left) or population (right). **A)** The top
333 candidate identified by SLRfinder. **B)** The single LD cluster identified on the sex chromosomes
334 **C & D)** Plots using SNPs from the two previously reported SLR candidates (Fraser et al.,
335 2020). The two sexes did not differ in heterozygosity, and the PC1 divergence mostly reflects
336 population structure.

337

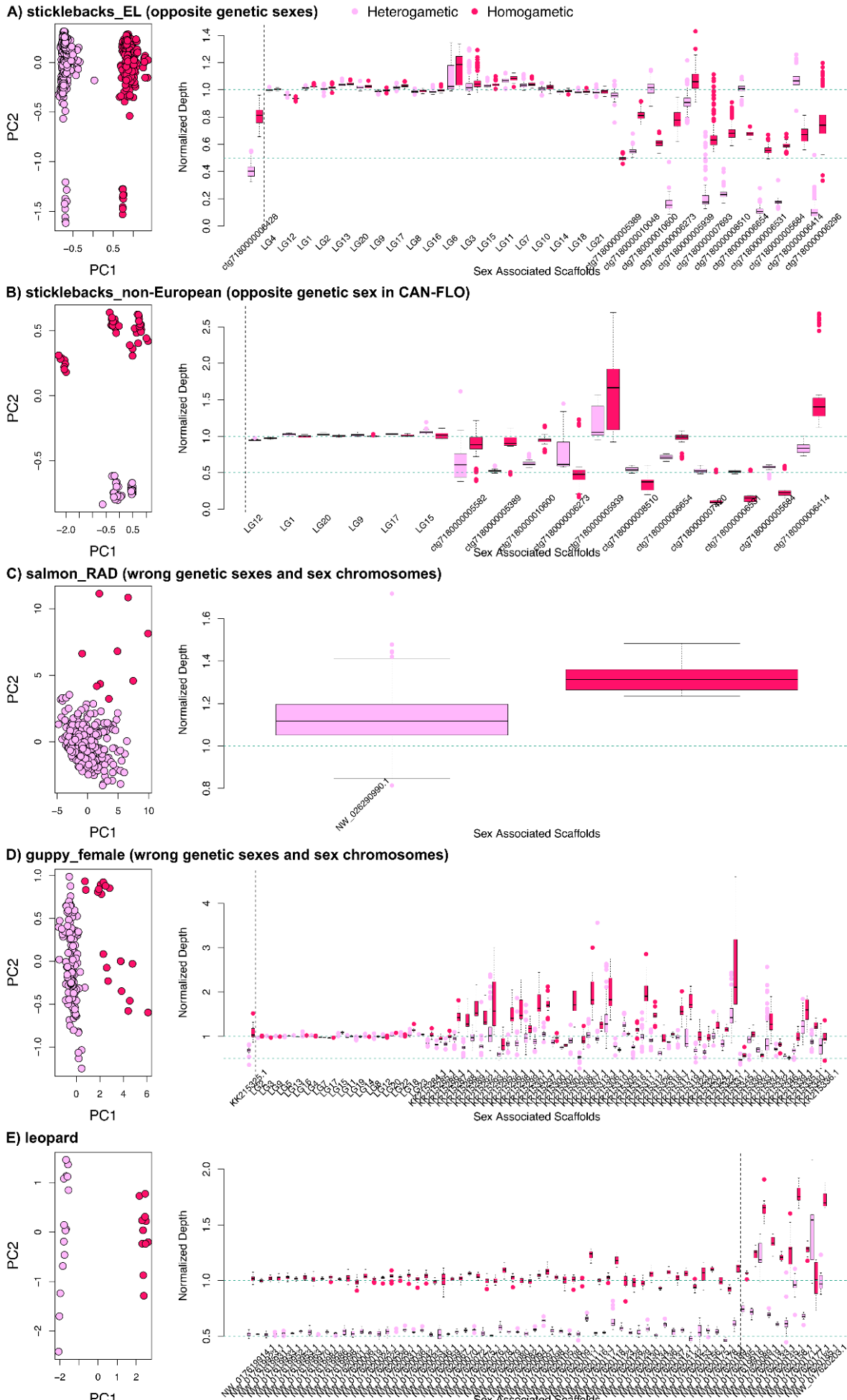
338 SLRfinder also did not find significant candidates in the dataset of African leopards, using the SATC-
339 inferred genetic sex and the PCA-inferred genetic populations (Fig. S3A). However, six LD clusters
340 were detected by filtering the misplaced sexes (Fig. S3B) and two of them were located on the
341 scaffolds that were also identified with abnormal depth ratios in SATC (see below), indicating that
342 these clusters are likely truly sex-linked.

343 *SATC analyses of test datasets*

344 SATC could not analyze the datasets of WL sticklebacks, UK sticklebacks, chum salmon mapped to
345 the female reference, or guppies mapped to the male reference genome. Specifically, when using the
346 *sexDetermine* command to identify sex and sex scaffolds in these datasets, SATC reported an error of
347 no good candidates found based on the depth of coverage, which is consistent with the previously
348 shown lack of differentiation of depth between sexes in most of these populations (Fraser et al., 2020;
349 Yi et al., 2024). Although SATC was able to process the chum salmon RAD data mapped to the male
350 reference genome and the guppy dataset mapped to the female reference genome, the inferred genetic
351 sexes were wrong and the known sex chromosomes could not be identified (Fig. 4CD), likely because
352 the chromosome-level depth difference was small and SATC could not break down long
353 chromosomes into small regions of SLRs.

354 When analyzing EL nine-spined sticklebacks, SATC inferred genetic sexes that were opposite to
355 phenotypic sexes or the previously identified genetic sexes (Yi et al., 2024), and wrongly identified a
356 putatively Y-linked unassembled contig (ctg7180000006428; Kivikoski et al., 2021) as X/Z-linked
357 (Fig. 4A). This is because SATC assumes only X/Z-linked contigs in the reference genome and
358 therefore always identifies the individuals having a higher depth of coverage on the sex-linked contigs
359 as the homogametic sex (Nursyifa et al., 2022). When the unassembled Y-contigs are included in the
360 reference genome, such as in the case of EL nine-spined sticklebacks (Kivikoski et al., 2021), these
361 contigs would show strong signals of low depth in XX females while high depth in XY males, which
362 would be misinterpreted by SATC assuming only X/Z-linked contigs. When analyzing non-European
363 sticklebacks, SATC did not detect X/Z-linked regions and only indicated several regions with
364 abnormal depth ratios (Fig. 4B). Interestingly, the SATC-inferred genetic sexes were consistent with
365 results from SLRfinder (Fig. 2C) and the previous study (Yi et al., 2024) in non-European
366 sticklebacks, except for a Canadian population (CAN-FLO) whose individuals were indicated as
367 genetic males in SLRfinder and in the previous study but genetic females in SATC. Additional
368 sampling with known phenotypic sexes is required to validate the sex identification of these non-
369 European populations. Overall, these results showed limited application of SATC to the identification
370 of labile sex chromosomes.

371 On the other hand, SATC was successfully applied to the dataset of African leopards which have
372 conserved sex chromosomes and were mapped to a scaffold-level female reference genome. Using
373 only 29 individuals, we identified 58 scaffolds as X/Z-linked and 8 scaffolds having abnormal depth
374 ratios (Fig. 4E), including all of the reported sex-linked scaffolds in previous studies using the same
375 dataset (Nursyifa et al., 2022; Pečnerová et al., 2021).



377 **Figure 4. SATC results of test datasets.** Colours represent the SATC-inferred homogametic (dark
378 red) and heterogametic (pink red) sexes. The left column is the PCA plot of the normalized depth of
379 coverage across all scaffolds and samples. The right column is the boxplot of the normalized depth of
380 coverage of each sex from the identified sex-linked scaffolds. The vertical dashed line separates the
381 scaffolds that passed both the t-test and ratio-based threshold (i.e., X/Z-linked, left to the line) from
382 those that only pass the t-test (i.e., abnormal depth ratios, right to the line).

383

384 *Power tests of SLRfinder*

385 Results of the power tests using the WL and EL sticklebacks are summarized in Table S2 and Table
386 S3, respectively. In the WL sticklebacks, SLRfinder accurately detected the LG3 SLR as the only
387 significant candidate when using all eight populations with three to five randomly selected individuals
388 per population (minimum 24 individuals in total). The LG3 SLR was always identified with the
389 lowest *p*-value when using one to five populations in the dataset, although only the test using five
390 populations showed significance. SLRfinder identified the LG3 SLR as the significant candidate when
391 testing the sex ratios (male:female) of 1:1 or 3:1 and with the lowest *p*-value when testing the sex
392 ratios of 1:2, 2:1, or 10:1. No significance was found and the LG3 SLR was not identified among top-
393 ranked candidates when testing the sex ratios 1:3 and 1:10 with the null expectation of even sex ratios.
394 We then set the expected sex ratio as 1:3 and 1:10 and re-ran SLRfinder on these datasets,
395 respectively. Tests of the sex ratio 1:3 with the corrected expectation and excluding the rank of
396 number of SNPs showed that the LG3 SLR had the lowest *p*-value (Table S2), but this result was not
397 significant (*p*=0.2) probably because few SNPs from the SLR were genotyped when few individuals
398 of the heterogametic sex were included in the samples. However, even if using the correct sex ratio
399 and no rank of number of SNPs, the LG3 SLR was not included in the top-ranked candidates when the
400 sex ratio was extremely skewed (1:10 or 10:1). The LG3 SLR was detected by filtering on the
401 percentage of misplaced sexes (based on the previously identified genetic sexes) in most of these
402 datasets. When one sex was completely missing, neither sex filtering nor the candidate ranking could
403 work and no false positives were found.

404 When applied to the EL sticklebacks, SLRfinder accurately detected the LG12 SLR as the only
405 significant candidate when using all 29 populations with three to five randomly selected individuals
406 per population, and when using three to five randomly selected populations (Table S3). When only
407 one population was included, the LG12 SLR was identified with a marginal *p*-value (0.08) as the top-
408 ranked candidate. However, when using two populations, the LG12 SLR was not included in the top-
409 ranked candidates, indicating some uncertainty when the sample size is small and the sex ratio is
410 uneven (around 1:3 in this case; using this sex ratio as the expectation allowed SLRfinder to add a

411 LG12 cluster to the top-ranked candidates). When testing different sex ratios, SLRfinder identified the
412 LG12 SLR as the significant candidate(s) using sex ratios of 1:1, 1:2, 2:1, 1:3, and 3:1. No
413 significance was found and the LG12 SLR was not identified among the top-ranked candidates when
414 using the most skewed sex ratios (1:10, 10:1). However, when providing the correct sex ratio of 10:1,
415 three significant candidates were detected, including the LG12 SLR and two false positives
416 ($p=0.0491$, Table S3). The LG12 SLR was detected by filtering based on the percentage of misplaced
417 sexes in all datasets except for those having the most skewed sex ratios (1:10, 10:1). Again, neither
418 sex filtering nor the candidate ranking could work when one sex was completely missing.

419

420 **Discussion**

421 Linkage disequilibrium (LD) has been shown to be highly informative about chromosomal evolution,
422 adaptation, and population structure (Kemppainen et al., 2015; Faria et al., 2019; Fang et al., 2020;
423 Fang et al., 2021; Guzmán et al., 2021), and has been also suggested to be potentially useful in
424 identifying SLRs (McKinney et al., 2020). However, signals of LD have remained under-exploited in
425 population genomic studies. Here we present a method, SLRfinder, which incorporates LD signals to
426 identify candidate SLRs and the sex chromosomes in which they are located. The results show that
427 SLRfinder successfully identified known SLRs as significant candidates when analyzing the
428 published population data of nine-spined sticklebacks and the chum salmon dataset mapped to the
429 male reference genome. In addition, using LD clustering, the SLRfinder-identified SLRs were
430 narrower than those identified using GWAS (Rondeau et al., 2023) or sliding windows (Yi et al.,
431 2024), which indicates that SLRfinder can be beneficial by further narrowing down the highly linked
432 SLR even when the pair of sex chromosomes is already known. Interestingly, the SLRs of nine-spined
433 sticklebacks and chum salmon have been indicated to involve genomic inversions (McKinney et al.,
434 2020; Natri et al., 2019; Yi et al., 2024) which might have strengthened the signals of LD and
435 heterozygosity detected in SLRfinder. Studies have proposed that structural variation, such as
436 inversions and chromosomal fusions, can facilitate recombination suppression in the newly formed
437 SLRs and thus may play important roles in early sex chromosome evolution (Kitano et al., 2009;
438 McKinney et al., 2020; Natri et al., 2019; Yi et al., 2024). However, it remains unclear how often
439 inversions (and other structural variants) might be associated with labile SLRs in natural populations.
440 We propose that SLRfinder might be helpful to answer this question as it is likely most sensitive to
441 the SLRs having structural variants and can be easily applied to genomic data of non-model
442 populations.

443 We compared SLRfinder, which is based on heterozygosity and mainly developed for labile sex
444 chromosomes, to the previously developed method SATC that is based on the depth of coverage

445 (Nursyifa et al., 2022). As expected, SLRfinder outperformed SATC in analysing labile sex
446 chromosomes that tend to have similar depths between sexes, such as in the WL sticklebacks and
447 chum salmon. In addition, SATC assumes no Y/W-linked scaffolds in the reference genome, which is
448 usually true in the taxa having conserved sex chromosomes because the highly degenerated Y/W
449 chromosomes are difficult to assemble and often excluded when the reference genome comes from
450 the heterogametic sex. However, reference genomes of the taxa having labile sex chromosomes are
451 more likely a mosaic combination of scaffolds from both sex chromosomes if the sequences were
452 from a heterogametic individual (e.g., the version 7 reference of the nine-spined stickleback;
453 Kivikoski et al., 2021), making SATC less applicable and even misleading (such as in the case of EL
454 sticklebacks). In addition, SATC was designed for data mapped to scaffold-level reference genomes
455 (Nursyifa et al., 2022) and could not break down long assembled chromosomes, which may prevent
456 the identification of narrow SLRs of labile sex chromosomes when using chromosome-level reference
457 genomes. On the other hand, SATC worked better than SLRfinder on conserved sex chromosomes
458 having clear inter-sex differences in the depth of coverage. Accordingly, our study suggests that
459 SLRfinder and SATC are complementary methods that specialize on different types of sex
460 chromosomes and datasets (**Table 2**). Therefore, we recommend testing both methods (and potentially
461 other methods as well) when trying to identify SLRs in new populations or species to get
462 complementary results.

463

464 **Table 2. Comparison between SLRfinder and SATC.**

	SLRfinder	SATC
Recommended type of sex chromosomes	Labile	Conserved
Considered signals	Linkage disequilibrium, number of SNPs in the LD cluster, heterozygosity, genetic differentiation	Depth of coverage
Sequencing data	Whole-genome resequencing (preferred) or restriction site-associated DNA sequencing	Whole-genome resequencing
Reference genome	Best if chromosome-level; homogametic or heterogametic sex	Best if scaffold-level; homogametic sex (no Y/W-linked scaffolds)
Phenotypic sex	Not required but can be incorporated to provide extra supports	Not required and not used.
Computational burden	Medium: memory and speed depend on data size	Small

465

466 Both SATC and SLRfinder do not require phenotypic sexes which can be difficult to obtain from non-
467 invasive sampling or difficult to identify without clear phenotypic sexual dimorphism. Instead, SATC
468 and SLRfinder can be used for genetic sex identification in addition to identifying candidate SLRs and
469 sex chromosomes. Furthermore, SLRfinder also has several advantages as illustrated in our analyses.
470 First, SLRfinder does not require known sex determination systems or a specific reference genome
471 from the heterogametic or homogametic sex. In our study we only tested taxa having the XX/XY
472 system but the same should apply to ZZ/ZW systems. It is worth noting that SLRfinder may work
473 better using the chromosome-level than the scaffold-level reference genome because the former
474 generates more and larger LD clusters. Second, SLRfinder does not require a specific sequencing
475 method (e.g., WGS or RADseq) and can be easily applied to any SNP genotypes in the VCF format.
476 The highly flexible R scripts allow manual parameter settings (e.g., *min_LD*, expected sex ratio, rank
477 parameters) and can be easily extended to include additional ranking or filtering parameters (e.g., F_{ST}
478 between sexes). Third, SLRfinder is a conservative method. Our test found very few false positives
479 which could be identified by the separation between phenotypic sexes and the usually higher *p*-values
480 than the top-ranked true SLRs. On the other hand, SLRfinder did not have enough power to detect
481 significant SLRs in several cases but the false negatives can be identified by filtering the misplaced
482 sexes. In addition, false negatives tend to be the top-ranked clusters with the lowest non-significant *p*-
483 values and the largest numbers of SNPs.

484 Like all the other methods, SLRfinder also has its limitations which were explored using the test
485 datasets. First, SLRfinder may have limited power when sample sizes are small, especially with a
486 limited number of populations. For example, SLRfinder successfully identified the true SLR using as
487 few as 24 individuals from eight WL populations of nine-spined sticklebacks, but not when using as
488 many as 79 individuals from 4 WL populations (Table S2). This is likely because more diverse
489 populations generate more and larger LD clusters, which increases the power of SLRfinder. Second,
490 SLRfinder requires sampling both sexes in relatively equal proportions. Although slightly skewed sex
491 ratios (max 1:3 or 3:1) could work in most cases and can be accounted for in χ^2 tests, SLRfinder
492 appears not to work when sex ratios are highly skewed (e.g., 1:10 or 10:1). However, although not
493 tested here, these limitations from the sample size and sex ratio likely also apply to most of the other
494 methods for SLR identification with few exceptions (e.g., FindZX may work on a single individual;
495 Sigeman et al., 2022).

496 Unsurprisingly, SLRfinder only works when the expected signals (differential heterozygosity and
497 genetic differentiation between sexes in SLRs) are present in the data. However, these signals may not
498 be clear in every dataset. When sample sizes are small and include low signal-to-noise ratios, these
499 expected signals can occur by chance rather than driven by linkage to sex. In addition, some
500 biological systems may exhibit complicated signals in their SLRs. For example, guppies showed no

501 difference in male and female heterozygosity and stronger population structure than inter-sex
502 divergence in the previously identified candidate SLRs (Fig. 3CD). The high heterozygosity in both
503 sexes and strong population signal might be explained by the maintenance of many different Y
504 haplotypes among these populations via balancing selection (Fraser et al., 2020). Similarly, a
505 previously developed coverage-based method, RADSex, was applied to 15 teleost fishes having labile
506 sex chromosomes but only six were successfully identified with sex markers (Feron et al., 2021).
507 Taken together, these results show that no single method is universally applicable to all taxa having
508 diverse sex chromosome systems.

509 In summary, SLRfinder provides a novel approach for the identification of labile sex chromosomes in
510 non-model populations using LD and heterozygosity. Given the lack of a universal method for
511 identifying SLRs across diverse sex chromosome systems, SLRfinder complements the previously
512 developed methods (e.g., SATC) by serving the same purpose in different contexts. SLRfinder seems
513 to work best when applied to a large number of divergent populations and when sex ratios are
514 relatively equal. It should be noted that the identified regions are candidate SLRs and putative sex
515 chromosomes which need to be further validated with additional data and other approaches. In
516 addition, SLRfinder is sensitive to inversions in SLRs (e.g., the LG12 and LG3 SLRs in sticklebacks)
517 and can detect autosomal regions that may have become sex-linked (e.g., the LG3 region in chum
518 salmon), which can be interesting in the contexts of sexual selection and antagonism.

519

520 **Acknowledgment and Funding**

521 We thank Dr. Bonnie Fraser for the help to get access to the raw data of guppies. This study was
522 supported by National Natural Science Foundation of China/Research Grants Council (RGC) Joint
523 Research Scheme 2021/2022 ('N_HKU763/21' to JM). We are grateful for the IT Centre for
524 Scientific Computing (CSC), Finland, for access to computing resources.

525

526 **References**

527 Blaser, O., Neuenschwander, S., & Perrin, N. (2014). Sex-chromosome turnovers: the hot-
528 potato model. *American Naturalist*, 183(1), 140–146. <https://doi.org/10.1086/674026>
529 Csardi, G., Nepusz, T., & others. (2006). The igraph software package for complex network
530 research. *InterJournal, Complex Systems*, 1695(5), 1–9.
531 Danecek, P., Auton, A., Abecasis, G., Albers, C. A., Banks, E., DePristo, M. A., Handsaker,
532 R. E., Lunter, G., Marth, G. T., Sherry, S. T., McVean, G., Durbin, R., & 1000
533 Genomes Project Analysis Group. (2011). The variant call format and VCFtools.
534 *Bioinformatics*, 27(15), 2156–2158. <https://doi.org/10.1093/bioinformatics/btr330>

535 Danecek, P., Bonfield, J. K., Liddle, J., Marshall, J., Ohan, V., Pollard, M. O., Whitwham,
536 A., Keane, T., McCarthy, S. A., Davies, R. M., & Li, H. (2021). Twelve years of
537 SAMtools and BCFtools. *GigaScience*, 10(2), giab008.
538 <https://doi.org/10.1093/gigascience/giab008>

539 Depristo, M. A., Banks, E., Poplin, R., Garimella, K. V., Maguire, J. R., Hartl, C.,
540 Philippakis, A. A., Del Angel, G., Rivas, M. A., Hanna, M., McKenna, A., Fennell, T.
541 J., Kurnytsky, A. M., Sivachenko, A. Y., Cibulskis, K., Gabriel, S. B., Altshuler, D.,
542 & Daly, M. J. (2011). A framework for variation discovery and genotyping using
543 next-generation DNA sequencing data. *Nature Genetics* 2011 43:5, 43(5), 491–498.
544 <https://doi.org/10.1038/ng.806>

545 Devlin, B., & Roeder, K. (1999). Genomic control for association studies. *Biometrics*, 55(4),
546 997–1004. <https://doi.org/10.1111/j.0006-341X.1999.00997.x>

547 Devlin, B., Roeder, K., & Wasserman, L. (2001). Genomic control, a new approach to
548 genetic-based association studies. *Theoretical Population Biology*, 60(3), 155–166.
549 <https://doi.org/10.1006/tpbi.2001.1542>

550 Dixon, G., Kitano, J., & Kirkpatrick, M. (2019). The origin of a new sex chromosome by
551 introgression between two stickleback fishes. *Molecular Biology and Evolution*,
552 36(1), 28–38. <https://doi.org/10.1093/MOLBEV/MSY181>

553 Dufresnes, C., Borzee, A., Horn, A., Stock, M., Ostini, M., Sermier, R., Wassef, J.,
554 Litvinchuk, S. N., Kosch, T. A., Waldman, B., Jang, Y., Brelsford, A., & Perrin, N.
555 (2015). Sex-chromosome homomorphy in Palearctic tree frogs results from both
556 turnovers and X–Y recombination. *Molecular Biology and Evolution*, 32(9), 2328–
557 2337. <https://doi.org/10.1093/MOLBEV/MSV113>

558 Faria, R., Chaube, P., Morales, H. E., Larsson, T., Lemmon, A. R., Lemmon, E. M.,
559 Rafajlović, M., Panova, M., Ravinet, M., Johannesson, K., Westram, A. M., & Butlin,
560 R. K. (2019). Multiple chromosomal rearrangements in a hybrid zone between
561 *Littorina saxatilis* ecotypes. *Molecular Ecology*, 28(6), 1375–1393.
562 <https://doi.org/10.1111/mec.14972>

563 Fang, B., Kemppainen, P., Momigliano, P., Feng, X., & Merilä, J. (2020). On the causes of
564 geographically heterogeneous parallel evolution in sticklebacks. *Nature Ecology &
565 Evolution*, 4(8), 1105–1115. <https://doi.org/10.1038/s41559-020-1222-6>

566 Fang, B., Kemppainen, P., Momigliano, P., & Merilä, J. (2021). Population structure limits
567 parallel evolution in sticklebacks. *Molecular Biology and Evolution*, 38(10), 4205–
568 4221. <https://doi.org/10.1093/MOLBEV/MSAB144>

569 Feng, X., Merilä, J., & Löytynoja, A. (2022). Complex population history affects admixture
570 analyses in nine-spined sticklebacks. *Molecular Ecology*, 31(20), 5386–5401.
571 <https://doi.org/10.1111/MEC.16651>

572 Feron, R., Pan, Q., Wen, M., Imarazene, B., Jouanno, E., Anderson, J., Herpin, A., Journot,
573 L., Parrinello, H., Klopp, C., Kottler, V. A., Roco, A. S., Du, K., Kneitz, S., Adolfi,
574 M., Wilson, C. A., McCluskey, B., Amores, A., Desvignes, T., ... Guiguen, Y.
575 (2021). RADSex: a computational workflow to study sex determination using
576 restriction site-associated DNA sequencing data. *Molecular Ecology Resources*,
577 21(5), 1715–1731. <https://doi.org/10.1111/1755-0998.13360>

578 Fraser, B. A., Whiting, J. R., Paris, J. R., Weadick, C. J., Parsons, P. J., Charlesworth, D.,
579 Bergero, R., Bemm, F., Hoffmann, M., Kottler, V. A., Liu, C., Dreyer, C., & Weigel,
580 D. (2020). Improved reference genome uncovers novel sex-linked regions in the
581 guppy (*Poecilia reticulata*). *Genome Biology and Evolution*, 12(10), 1789–1805.
582 <https://doi.org/10.1093/GBE/EVAA187>

583 Furman, B. L. S., Metzger, D. C. H., Darolti, I., Wright, A. E., Sandkam, B. A., Almeida, P.,
584 Shu, J. J., Mank, J. E., & Fraser, B. (2020). Sex chromosome evolution: so many

585 exceptions to the rules. *Genome Biology and Evolution*, 12(6), 750–763.
586 <https://doi.org/10.1093/gbe/evaa081>

587 Guzmán, N. V., Kemppainen, P., Monti, D., Castillo, E. R. D., Rodriguero, M. S., Sánchez-
588 Restrepo, A. F., Cigliano, M. M., & Confalonieri, V. A. (2022). Stable inversion
589 clines in a grasshopper species group despite complex geographical history.
590 *Molecular Ecology*, 31(4), 1196–1215. <https://doi.org/10.1111/mec.16305>

591 Jeffries, D. L., Lavanchy, G., Sermier, R., Sredl, M. J., Miura, I., Borzée, A., Barrow, L. N.,
592 Canestrelli, D., Crochet, P. A., Dufresnes, C., Fu, J., Ma, W. J., Garcia, C. M., Ghali,
593 K., Nicieza, A. G., O'Donnell, R. P., Rodrigues, N., Romano, A., Martínez-Solano,
594 Í., ... Perrin, N. (2018). A rapid rate of sex-chromosome turnover and non-random
595 transitions in true frogs. *Nature Communications*, 9(1), 1–11.
596 <https://doi.org/10.1038/s41467-018-06517-2>

597 Jeffries, D. L., Mee, J. A., & Peichel, C. L. (2022). Identification of a candidate sex
598 determination gene in *Culaea inconstans* suggests convergent recruitment of an *Amh*
599 duplicate in two lineages of stickleback. *Journal of Evolutionary Biology*, 35(12),
600 1683–1695. <https://doi.org/10.1111/JEB.14034>

601 Kemppainen, P., Knight, C. G., Sarma, D. K., Hlaing, T., Prakash, A., Maung Maung, Y. N.,
602 Somboon, P., Mahanta, J., & Walton, C. (2015). Linkage disequilibrium network
603 analysis (LDna) gives a global view of chromosomal inversions, local adaptation and
604 geographic structure. *Molecular Ecology Resources*, 15(5), 1031–1045.
605 <https://doi.org/10.1111/1755-0998.12369>

606 Kitano, J., Ansai, S., Fujimoto, S., Kakioka, R., Sato, M., Mandagi, I. F., Sumarto, B. K. A.,
607 & Yamahira, K. (2023). A cryptic sex-linked locus revealed by the elimination of a
608 master sex-determining locus in medaka fish. *The American Naturalist*, 202(2), 231–
609 240. <https://doi.org/10.1086/724840>

610 Kitano, J., Ross, J. A., Mori, S., Kume, M., Jones, F. C., Chan, Y. F., Absher, D. M.,
611 Grimwood, J., Schmutz, J., Myers, R. M., Kingsley, D. M., & Peichel, C. L. (2009). A
612 role for a neo-sex chromosome in stickleback speciation. *Nature*, 461(7267), 1079–
613 1083. <https://doi.org/10.1038/nature08441>

614 Kivikoski, M., Rastas, P., Löytynoja, A., & Merilä, J. (2021). Automated improvement of
615 stickleback reference genome assemblies with Lep-Anchor software. *Molecular
616 Ecology Resources*, 21(6), 2166–2176. <https://doi.org/10.1111/1755-0998.13404>

617 Kü Nstner, A., Hoffmann, M., Fraser, B. A., Kottler, V. A., Sharma, E., Weigel, D., &
618 Dreyer, C. (2016). The genome of the Trinidadian guppy, *Poecilia reticulata*, and
619 variation in the Guanapo population. *PLOS ONE*.
620 <https://doi.org/10.1371/journal.pone.0169087>

621 Li, H. (2011). A statistical framework for SNP calling, mutation discovery, association
622 mapping and population genetical parameter estimation from sequencing data.
623 *Bioinformatics*, 27(21), 2987–2993.
624 <https://doi.org/10.1093/BIOINFORMATICS/BTR509>

625 Li, H. (2013). Aligning sequence reads, clone sequences and assembly contigs with BWA-
626 MEM (arXiv:1303.3997). arXiv. <https://doi.org/10.48550/arXiv.1303.3997>

627 Ma, J., & Amos, C. I. (2012). Investigation of inversion polymorphisms in the human
628 genome using principal components analysis. *PLoS ONE*, 7(7), 40224–40224.
629 <https://doi.org/10.1371/journal.pone.0040224>

630 McKinney, G., McPhee, M. V., Pascal, C., Seeb, J. E., & Seeb, L. W. (2020). Network
631 analysis of linkage disequilibrium reveals genome architecture in chum salmon. *G3
632 Genes|Genomes|Genetics*, 10(5), 1553–1561. <https://doi.org/10.1534/G3.119.400972>

633 Natri, H. M., Merilä, J., & Shikano, T. (2019). The evolution of sex determination associated
634 with a chromosomal inversion. *Nature Communications*, 10(1), 1–13.

635 https://doi.org/10.1038/s41467-018-08014-y
636 Nursyifa, C., Brüniche-Olsen, A., Garcia-Erill, G., Heller, R., & Albrechtsen, A. (2022). Joint
637 identification of sex and sex-linked scaffolds in non-model organisms using low depth
638 sequencing data. *Molecular Ecology Resources*, 22(2), 458–467.
639 https://doi.org/10.1111/1755-0998.13491
640 Palmer, D. H., Rogers, T. F., Dean, R., & Wright, A. E. (2019). How to identify sex
641 chromosomes and their turnover. *Molecular Ecology*, 28(21), 4709–4724.
642 https://doi.org/10.1111/MEC.15245
643 Pečnerová, P., Garcia-Erill, G., Liu, X., Nursyifa, C., Waples, R. K., Santander, C. G., Quinn,
644 L., Frandsen, P., Meisner, J., Stæger, F. F., Rasmussen, M. S., Brüniche-Olsen, A.,
645 Hviid Friis Jørgensen, C., da Fonseca, R. R., Siegismund, H. R., Albrechtsen, A.,
646 Heller, R., Moltke, I., & Hanghøj, K. (2021). High genetic diversity and low
647 differentiation reflect the ecological versatility of the African leopard. *Current
648 Biology*, 31(9), 1862-1871.e5. https://doi.org/10.1016/J.CUB.2021.01.064
649 Perrin, N. (2021). Sex-chromosome evolution in frogs: What role for sex-antagonistic genes?
650 *Philosophical Transactions of the Royal Society B*, 376(1832).
651 https://doi.org/10.1098/RSTB.2020.0094
652 R Core Team. (2022). R: A language and environment for statistical computing. *R
653 Foundation for Statistical Computing*. Vienna, Austria. <https://www.R-project.org/>.
654 Rochette, N. C., Rivera-Colón, A. G., & Catchen, J. M. (2019). Stacks 2: Analytical methods
655 for paired-end sequencing improve RADseq-based population genomics. *Molecular
656 Ecology*, 28(21), 4737–4754. https://doi.org/10.1111/MEC.15253
657 Rondeau, E. B., Christensen, K. A., Johnson, H. A., Sakhraei, D., Biagi, C. A., Wetklo, M.,
658 Despins, C. A., Leggatt, R. A., Minkley, D. R., Withler, R. E., Beacham, T. D., Koop,
659 B. F., & Devlin, R. H. (2023). Insights from a chum salmon (*Oncorhynchus keta*)
660 genome assembly regarding whole-genome duplication and nucleotide variation
661 influencing gene function. *G3 Genes|Genomes|Genetics*, 13(8).
662 https://doi.org/10.1093/G3JOURNAL/JKAD127
663 Sigeman, H., Sinclair, B., & Hansson, B. (2022). Findzx: an automated pipeline for detecting
664 and visualising sex chromosomes using whole-genome sequencing data. *BMC
665 Genomics*, 23(1), 1–14. https://doi.org/10.1186/S12864-022-08432-9/FIGURES/5
666 Tree of Sex Consortium. (2014). *Tree of sex: A database of sexual systems* [dataset]. Nature
667 Publishing Group. <https://doi.org/10.5061/DRYAD.V1908>
668 Van der Auwera, G. A., Carneiro, M. O., Hartl, C., Poplin, R., del Angel, G., Levy-
669 Moonshine, A., Jordan, T., Shakir, K., Roazen, D., Thibault, J., Banks, E., Garimella,
670 K. V., Altshuler, D., Gabriel, S., & DePristo, M. A. (2013). From fastQ data to high-
671 confidence variant calls: the genome analysis toolkit best practices pipeline. *Current
672 Protocols in Bioinformatics*, 43(1), 11.10.1-11.10.33.
673 https://doi.org/10.1002/0471250953.BI1110S43
674 Vicoso, B. (2019). Molecular and evolutionary dynamics of animal sex-chromosome
675 turnover. *Nature Ecology and Evolution*, 3(12), 1632–1641.
676 https://doi.org/10.1038/s41559-019-1050-8
677 Yi, X., Wang, D., Reid, K., Feng, X., Löytynoja, A., & Merilä, J. (2024). *Sex chromosome
678 turnover in hybridizing stickleback lineages* (p. 2023.11.06.565909). bioRxiv.
679 https://doi.org/10.1101/2023.11.06.565909
680 Zheng, X., Levine, D., Shen, J., Gogarten, S. M., Laurie, C., & Weir, B. S. (2012). A high-
681 performance computing toolset for relatedness and principal component analysis of
682 SNP data. *Bioinformatics*, 28(24), 3326–3328.
683 https://doi.org/10.1093/BIOINFORMATICS/BTS606
684

685 **Data availability**

686 SLRfinder scripts are publicly available on GitHub (<https://github.com/xuelingyi/SLRfinder>) with a
687 step-by-step tutorial. The sample information of our tested datasets are also provided on GitHub.

688

689 **Author Contribution**

690 P.K. and X.Y. conceptualized the study. P.K. designed the method and wrote the raw scripts. X.Y.
691 polished the method and analyzed empirical datasets. J.M. supervised the study and provided
692 resources. X.Y. and P.K. drafted the manuscript. All authors edited the manuscript.

693

694 **Conflict of Interest**

695 The authors claim no conflict of interest.

696